Rapid, global demographic expansions after the origins of agriculture

Christopher R. Gignoux[a,1,2], Brenna M. Henn[b,1,3], and Joanna L. Mountain[b,c]

[a]University of California, San Francisco, CA 94158; [b]Department of Anthropology, Stanford University, Stanford, CA 94305; and [c]23andMe, Inc., Mountain View, CA 94043

Edited by Ofer Bar-Yosef, Harvard University, Cambridge, MA, and approved February 18, 2011 (received for review January 8, 2010)

The invention of agriculture is widely assumed to have driven recent human population growth. However, direct genetic evidence for population growth after independent agricultural origins has been elusive. We estimated population sizes through time from a set of globally distributed whole mitochondrial genomes, after separating lineages associated with agricultural populations from those associated with hunter-gatherers. The coalescent-based analysis revealed strong evidence for distinct demographic expansions in Europe, southeastern Asia, and sub-Saharan Africa within the past 10,000 y. Estimates of the timing of population growth based on genetic data correspond neatly to dates for the initial origins of agriculture derived from archaeological evidence. Comparisons of rates of population growth through time reveal that the invention of agriculture facilitated a fivefold increase in population growth relative to more ancient expansions of hunter-gatherers.

Holocene | Neolithic | Phylogenetics

Beginning as early as 12 thousand years ago (kya), multiple hunter-gatherer populations began developing agriculture and animal domestication. Food production quickly spread to neighboring regions (1). Discriminating between population dispersal (i.e., demic) and cultural diffusion models of agropastoral expansions has been a central topic in human population genetic research for >20 years. This effort has been complicated by difficulties in dating migratory events, assigning genetic types to geographic origins, and modeling complex demographic models with multiple migration waves.

Recent analyses of genetic variation in European populations have provided support for both types of models. Haak et al. (2) found, via analysis of ancient DNA, that early Neolithic farmers carried a mitochondrial lineage that is extremely rare among contemporary Europeans. They argued that the rarity of this lineage supports a model of cultural diffusion of agriculture, whereby Neolithic dispersals had little effect on the overall gene pool of Europeans. This cultural model can be contrasted with a demic diffusion model whereby agricultural populations from the Near East expanded into and throughout Europe during the Neolithic, initially remaining genetically isolated from indigenous hunter-gatherers. More recent ancient DNA work (3) indicates a "substantial influx" of agriculturist individuals from the Near East during the early Neolithic. The demic diffusion model has also been supported by Y-chromosomal, mitochondrial (mtDNA), and autosomal data (4–6) and has found some corroboration in a mixed model incorporating both Near Eastern migration and indigenous European acculturation (7). This demic vs. cultural diffusion debate is not limited to European prehistory. Recent population genetic research in eastern Asian, Indian, and African populations has generally favored demic diffusion models (8–10). However, prior studies were unable to provide concrete evidence of the timing or magnitude of the population growth associated with agriculture, in part because they did not discriminate between lineages of hunter-gatherer and agricultural origin.

Given recent suggestive support for demic diffusion models, we designed our study to account for possible separate population histories from indigenous hunter-gatherers and agriculturalists to ask related but previously unaddressed questions: Did the adoption of agriculture and pastoralism affect human population size (11)? If so, how does the rate of growth compare with prior population expansions? The majority of the population genetic research so far has focused on ancient events such as the Out-of-Africa expansion and regional time to the most recent common ancestor (TMRCA) estimates (11–13), but very few have used coalescent methodologies to investigate the impact of recent demographic events. Rejection–algorithm-based analyses using Y-chromosomal data support population expansion dating to the Last Glacial Period (LGP), although the wide credible intervals are not inconsistent with population growth during the Neolithic period (11, 13). Using mtDNA, Atkinson et al. (12) identified the Upper Paleolithic Out-of-Africa expansion as the defining period of human population growth. However, they were unable to detect expansions during the agricultural period (i.e., the Neolithic). Atkinson et al. attributed this absence to the technical limits of their method. However, if both agricultural and indigenous hunter-gatherer lineages are present in a dataset, the signal of agricultural growth could be masked. Previous coalescent-based sensitivity analysis of Y-chromosome data has shown the confounding effect of complex population history on expansion time inference: Mixed samples will reflect the older expansion event (14).

Results

To circumvent the problem of older demographic events obscuring recent events (14), we partitioned sets of major mtDNA haplogroups into three climatic time periods for analysis according to their prior TMRCA estimates: Holocene, LGP, and Upper Paleolithic (0–12 kya, 12–25 kya, 25–50 kya). The time of origin (TMRCA) and time of fastest population growth for a given haplogroup need not, and often do not, coincide (12, 15). We first sorted mtDNA lineages according to their present geographic distribution, focusing on Europe, southeastern Asia, and sub-Saharan Africa because agriculture was uniquely innovated in each region. Each geographic dataset was divided into two subsets, a Holocene set and a LGP or Upper Paleolithic set. Representatives of multiple major haplogroups were included

Author contributions: C.R.G. and B.M.H. designed research; C.R.G. and B.M.H. performed research; C.R.G. and B.M.H. contributed new reagents/analytic tools; C.R.G., B.M.H., and J.L.M. analyzed data; and C.R.G., B.M.H., and J.L.M. wrote the paper.

The authors declare no conflict of interest.

This article is a PNAS Direct Submission.

Data deposition: The sequences reported in this paper are publicly available in the GenBank database (accession nos. available in *SI Materials and Methods*).

[1]C.R.G. and B.M.H. contributed equally to this work.

[2]To whom correspondence should be addressed: E-mail: chris.gignoux@ucsf.edu.

[3]Present address: Department of Genetics, Stanford University, Stanford, CA 94305.

This article contains supporting information online at www.pnas.org/lookup/suppl/doi:10.1073/pnas.0914274108/-/DCSupplemental.

in each sample set to avoid lineage-specific effects; the inclusion of multiple major haplogroups allows us to identify a common signal of the timing of population growth.

To discriminate between demic and cultural diffusion hypotheses, we required that the Holocene haplogroups be previously associated with an origin in a geographic center of agricultural diffusion (i.e., the Near East, southeastern Asia, and western Africa). The criteria for haplogroup partitioning were based on previously published research; generally other researchers have argued that haplogroups with greater genetic diversity near the site of agricultural innovation may be associated with demic diffusion (*SI Materials and Methods*). After assembling the three geographic datasets, we had a total of 425 mtDNA coding region sequences, comprising >6 Mb of sequence data. We then estimated effective population size through time via coalescent Bayesian Skyline plots (16) to infer population size during the LGP and Holocene, and compared our indigenous Paleolithic lineages to Holocene migrants, correcting for the established time dependency (non–clock-like behavior) of mitochondrial mutation rates (17, 18). As has been shown , the nonparametric Bayesian Skyline approach can resolve recent population growth events (12, 18–21). Furthermore, because we combine multiple mtDNA haplogroups for each Holocene/Upper Paleolithic dataset, Skyline analysis could also reflect more ancient events, given that the coalescence of multiple Out-of-Africa haplogroups within a set is generally 40,000–60,000 y ago (22) (Fig. S1).

European Population Growth. We found that Europeans with Holocene-era haplogroups of proposed Near Eastern origin experienced a major population growth phase during the agricultural transition (Fig. 1*A*). Early calibrated radiocarbon dates of Neolithic agricultural remains from eastern and central Europe date to ≈8,000 ya (Fig. 2*A*). The genetic-based European Holocene Skyline begins to grow rapidly by 7,700 ya (CI: 6,500–9,000 ya) (Fig. 1*A* and Table 1), concordant with the timing of the introduction of agriculture to central Europe (outside the Balkans and Anatolia) (23).

In contrast, our dataset of lineages indigenous to Europe from the LGP does not show the same marked expansion during the agricultural period. Our European LGP dataset shows a relatively slow expansion beginning ≈12,000 ya (Fig. 1*A* and Table 1), matching the timing for the Younger Dryas glacial cycle. Expansion from southern refugia ≈15,000 ya was stalled by this cycle, a short period of intense cold, from ≈12,900 to 11,500 ya (24). The expansion of hunter-gatherers from southern Europe following the Younger Dryas supports the hypothesis that the LGP played a role in shaping patterns of European genetic diversity (25, 26).

African Population Growth. We find two periods of population expansion within our sample of lineages originating during the Holocene in western Africa. Although the majority of coalescent events occur during the Holocene, a number of lineages from this sample also coalesce during the Upper Paleolithic. The earliest growth begins at ≈38,000 ya (CI: 33,500–45,000 ya) (Table 1 and Fig. S1) and the second period begins at ≈4,600 ya (CI: 3,000–10,000 ya) (Table 1 and Fig. 1*B*). The correspondence between the timing of genetic evidence for a sharp increase in population size at 4,600 ya in our Holocene sample of sub-Saharan Africans and the archaeological evidence for origins of agriculture in western Africa is quite close (Fig. 1*B* and Table 1). In contrast, our southern African Upper Paleolithic sample representative of hunter-gatherers shows no growth over the past 20,000 y. We suggest Bantu-speaking farmers and other pastoralist groups migrated throughout southern Africa 2,000 ya (27) without impacting southern African mtDNA lineages (Fig. 1*B*).

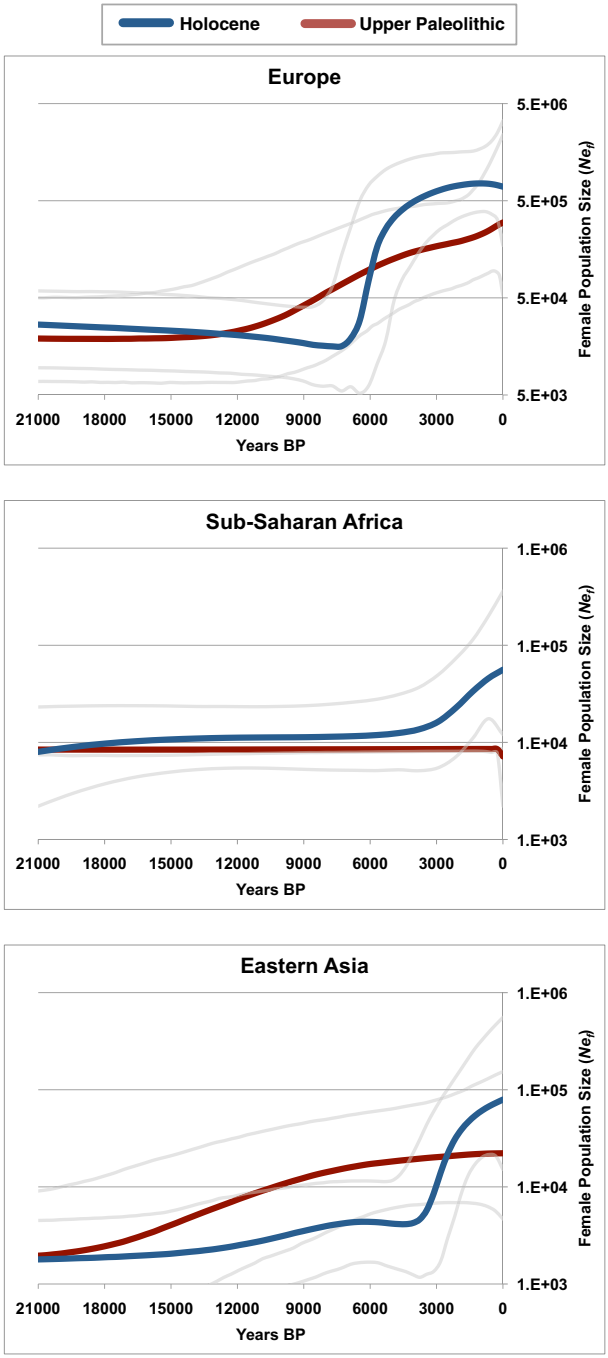

Fig. 1. Bayesian Skyline plots showing estimates of the effective size of the female population through time, given mtDNA lineages from both the Holocene and Upper Paleolithic: European Holocene and Upper Paleolithic population size curves (*Top*), sub-Saharan African Holocene and Upper Paleolithic population size curves (*Middle*), Southeastern Asia Holocene and Papua New Guinea Upper Paleolithic population size curves (*Bottom*). For each point in time, the median female population effective size is plotted along with the 95% confidence intervals. Because each set of lineages represents a fraction of the lineages present in each region, size estimates are also only a fraction of the actual population size. Y axes are adjusted for clarity. The *x* axis represents time in years. Skyline curves were independently corrected for the time dependency of mtDNA mutation rate estimates to accurately compare the timing of genetic growth estimates and archaeological dates for population events.

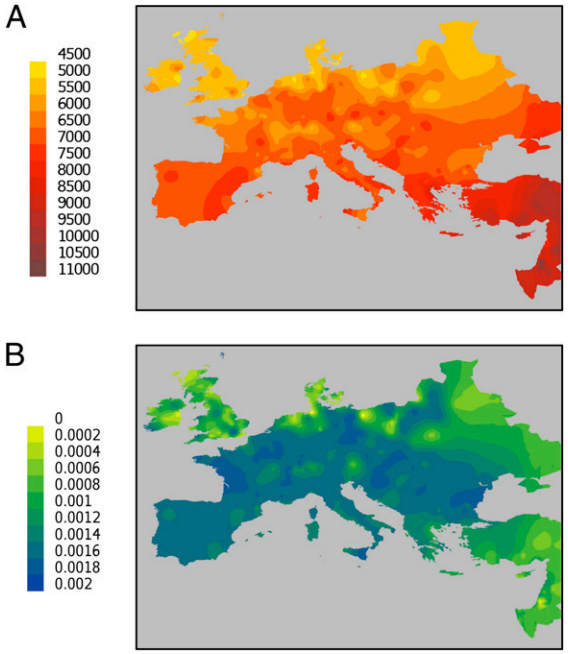

Fig. 2. Map showing the rate of agricultural population growth for Europe interpolated via Kriging from archaeological data on the Neolithic incursion. (*A*) The dates of the initial Neolithic (agricultural) remains based on 665 calibrated radiocarbon archaeological sites from Pinhasi et al. (23). Units are in years. (*B*) The timing of each archaeological site was then paired with the appropriate population growth rate during the same time interval calculated from our European Neolithic Skyline analysis seen in Fig. 1 assuming a wavefront expansion. Darker colors indicate more rapid population growth; lighter colors indicate slower population growth. Initially, population growth in our European Holocene dataset was moderate. Only after agriculture diffused across the Mediterranean regions did population growth begin to accelerate (Fig. 2*B*).

Asian Population Growth. Our third region encompasses continental and island Southeastern Asia. Direct archaeological evidence for rice agriculture in southeastern Asia dates to only ≈4,400 ya in Thailand (28). Agriculture spread throughout Island Southeast Asia, with evidence of rice in Taiwan again dating to ≈4,400 ya. Our Southeastern Asian Holocene population size curve indicates expansion beginning ≈4,700 ya (CI: 3,000–5,700 ya) (Fig. 1*C* and Table 1). Subsequent migrations throughout Indonesia into coastal Papua New Guinea (PNG) and across Polynesia likely allowed for continued population growth up to the present day.

PNG is an independent location of agricultural innovation. Highland PNG populations developed wetland horticulture during the Holocene, by at least 7,000 ya (29). Our indigenous PNG Upper Paleolithic sample showed no unusual change in growth rate about that time (Fig. 1*C* and Table 1) (30), suggesting there was either no radical change in population size in early PNG populations or, because the small sample of lineages, we were unable to detect recent growth. Our analysis instead suggests that PNG population growth began ≈26,000 ya, from ≈1,700 women, and intensified throughout the LGP. Human-directed vegetative burning and the extinction of megafauna in the highlands both occurred during the LGP (31). The fastest population growth for Upper Paleolithic PNG lineages occurred ≈14,500 ya, corresponding to the initiation of a stable, global warming interval (24).

Rates of Population Growth. Our genetic estimates of the rate of population growth during the Holocene period in Europe, southeastern Asia, and western Africa are three to six times faster than earlier population expansions (Table 1). Our population growth rates compare favorably to those calculated by using other data sets (13, 32). The European samples show moderate population growth of 0.021% per year beginning 12,000 ya for the indigenous LGP lineages and rapid growth of 0.058% per year during the Holocene (Table 1). Estimates of growth rates for Holocene African agriculturalists, 0.03%, are lower than estimates for other regions (Table 1), consistent with Y-chromosomal results (13). Other researchers have pointed out the difficulty of developing systematic agriculture in sub-Saharan Africa compared with the other regions in our study (27). When we break down the Skyline curves to examine the growth rate by interval (300–500 y), the maximum growth rates follow a similar pattern (Table 1). The maximum growth rates from the Holocene period tend to be three to seven times faster than Upper Paleolithic expansions. Our Holocene population growth rate estimates, coupled with the correlation between population size changes and the onset of agriculture in each region, suggest that the switch to agriculture caused unusually high rates of population growth.

Discussion

Demic Diffusion of Agriculture in Europe. Demic and cultural diffusion models predict different demographic impacts on hunter-gatherer populations during the agricultural transition. If the indigenous hunter-gather Europeans had adopted agriculture by cultural diffusion, we would expect to see their growth rate accelerate beginning ≈8,000 ya, as we see for lineages associated

Table 1. Population growth rates calculated from skyline plots

Sample	Epoch,* Kya	First evidence of agriculture, ya	Growth began,† ya	95% CI for start of growth	Population growth rate, %	Fastest growth interval, ya	Maximum growth rate by interval, %
Europe Holocene	0–12	7,800	7,700	6,500–9,000	0.058	6,500–6,000	0.236
Europe Last Glacial	12–25		12,000	10,600–16,500	0.021	8,100–7,800	0.037
Western Africa Holocene	0–12	<5,000‡	4,600	3,000–10,000	0.032	2,100–1,400	0.052
Western Africa Upper Paleolithic§	12–50		38,000	33,500–45,000	0.007§	26,600–25,000	0.014
Southeast Asia Holocene	0–12	4,400	4,700	3,000–5,700	0.063	3,100–2,800	0.158
PNG Upper Paleolithic	12–50		21,000	17,000–26,500	0.011	14,700–14,400	0.021

*Period into which TMRCAs were partioned before applying Bayesian Skyline analysis.
†Years since population growth began. Calculated from the slowest acceleration interval until the present day.
‡Evidence from forest clearing. First evidence for crops at 3,500 kya.
§Our dataset of lineages from southern Africa with TMRCAs during the Upper Paleolithic showed no population growth. However, our western African Holocene dataset displayed two periods of growth: one during the Holocene and one during the Upper Paleoltihic. We present results from the western African Upper Paleolithic population growth, calculated from 38,000 ya until 13,600 ya, when growth reached stasis. See *SI Materials and Methods* for the extended western African population growth curve.

with agriculture. However, LGP European growth increases monotonically throughout the entire Holocene and there is no radical change in population growth rate (Fig. 1*A*). The absence of a distinct Holocene-period expansion suggests that the adoption of agriculture by indigenous hunter-gatherer Europeans was slow at best and did not contribute substantially to the initial geographic and demographic expansion of agriculture in Europe.

The samples in our dataset were from European populations living in mainland Europe (Table S1). If a demic diffusion event had involved massive population movement from the Near East, the European Holocene dataset would show an expansion time before 10,000 ya reflecting the earlier adoption of agriculture in the Near East. The concordance between dates inferred from our genetic data and archaeological dates from central Europe suggests that our European Holocene sample set largely contains lineages that are derived from a founding event of Near Eastern individuals. Thus, a relatively small number of Near Eastern founder individuals had a major genetic impact in Europe.

Archaeological evidence suggests that agricultural practices initially spread quickly across the Mediterranean regions of Europe (Fig. 2*A*). Linear regression on Neolithic archaeological sites across Europe suggests that agriculture diffused at a rate of ≈1 km/y (23, 33); however, this is contingent on a model of constant expansion from a point source in the Levant. Aligning the Holocene population growth rates calculated from Fig. 1*A* with the earliest archaeological evidence for agriculture at >600 sites in Europe, we can clearly see a two-phase Neolithic settlement of Europe (Fig. 2*B*). Initially, population growth in our European Holocene dataset was moderate. Only after agriculture diffused across the Mediterranean regions did population growth begin to accelerate (Fig. 2*B*). The fastest rate of European population growth occurred during the intermediate time period, of ≈6,500–6,000 ya. The later movement of agriculture into the northern latitudes of Europe correlates with a slower growth rate, due to colder climates and/or spatial restrictions.

Our results are consistent with recent publications using ancient DNA to assign the maternal affinities of early agriculturalists and hunter-gatherers. Our LGP European sample includes the U5a and U5b1 haplogroups, associated with Mesolithic hunter-gatherers at the majority of archaeological sites in Bramanti et al. (3) dated to older than 5,000 ya. The presence of similar mtDNA haplogroups in Mesolithic hunter-gatherers and contemporary Europeans supports a model involving (maternal) population continuity, even if this Mesolithic ancestry makes up only a fraction of contemporary European genomes. U5a, U5b1, V, and 3H combined account for ≈15% of western Europeans mtDNA haplogroups (7) (Table S1). Recent ancient DNA evidence has not yet resolved a dispute between models of demic diffusion and cultural diffusion agricultural practices, in part because the sample sizes and geographic sites of the two primary aDNA Neolithic studies are limited (2, 3).

Demographic Fluctuations in Western Africa. Present-day African farming populations likely trace much of their ancestry to western Africa, given the major impact of the recent expansion of Bantu-speaking farmers throughout much of sub-Saharan Africa (27). We restricted our selection of Holocene-period African lineages to those originating within western Africa (*SI Materials and Methods*) in order accurately detect early stages of agricultural population growth. The initial migration of Bantu speakers has been linked to the origins of agriculture (e.g., yam, oil palm) in the Congo Basin of Nigeria and Cameroon. These agricultural products tend to preserve poorly in the African rainforest, complicating precise archaeological dating of the origins of sub-Saharan agriculture. Evidence for the earliest domesticated pearl millet suggests a date of at least 3,500 ya (34). Other agricultural indicators, such as clearing of forest for oil palm, suggest western Africans may have begun cultivating food plants 5,000 ya or possibly earlier (27). The correspondence between a 3,500–5,000 ya origin of agriculture in western African and our estimates of the initiation of population growth among western African lineages at 4,600 ya is remarkably close (Table 1).

Our data from western African also suggest an early population expansion beginning at ≈38,000 ya and leveling off ≈20,000–15,000 ya (Fig. S1). The earlier expansion may be associated with the initial occupation of western Africa by modern humans, although the date when behaviorally modern humans appear in central/western Africa is debatable. However, our results are concordant with prior research on demographic change in individuals of western African descent. Zhivotovsky et al. (35) found a signature of population expansion in western Africans obtained from the Human Genome Diversity Panel (CEPH-HGDP) occurring at 35,000 ya and estimated from autosomal microsatellite data (35). Marth et al. (36) used >30,000 single-nucleotide polymorphisms (SNPs) to infer ancient population expansion in African-Americans that predated the growth in European and Asian samples. Resequencing data, from 40 unlinked autosomal loci, also indicated population growth in western Africa beginning 25,000–30,000 ya (depending on generation time) (37). It seems clear that our mtDNA and prior autosomal DNA estimates support a model of population growth in western Africa beginning only ≈40,000–30,000 ya.

Skyline Analysis Method. We characterize the timing of population growth in haplogroups originating within two broad climatic periods, the Holocene and either the LGP/or Upper Paleolithic, for lineages in Europe, southeastern Asia, and sub-Saharan Africa. We ask whether the time and magnitude of population growth estimates correlates with the transition to agriculture in each region. In theory, our coalescent Skyline analysis could show population growth occurring at any point, or not at all, during the Holocene. Additionally, the combination of haplogroups from divergent lineages in the mtDNA phylogeny (e.g., M and N lineages) allows for the possibility that the number of coalescent events could be concentrated in time intervals older than the Holocene. For example, our Holocene West African set of haplogroups shows both a recent expansion at 4,600 ya, consistent with growth at the time of invention of agriculture in central and western Africa; but the same set of haplogroups also shows population growth at 38,000 ya (Fig. S1). This result illustrates how our division of haplogroups does not restrict population growth to a particular period, as long as representatives from multiple major haplogroups are included in the analysis.

We observe the widening of confidence intervals in estimates of effective population size from ≈0–1,000 ya (Fig. 1 *A* and *B*) or 0–2,000 ya (Fig. 1*C*). This observation suggests that estimates of the timing of extremely recent population growth (within the last 1,000 y) and population size are likely unreliable, given the amount of time needed to accumulate mtDNA mutations. However, in this paper, we asked whether the origins of agriculture (occurring 4,000–12,000 ya) are associated with the timing of rapid population growth in our samples. Over the past ≈2,000 y, whole mtDNA genomes have accumulated sufficient mutations to estimate coalescent events reliably, based on distribution of 95% confidence intervals (Fig. 1 and Table 1).

Conclusions

To conclude, the Bayesian Skyline method is extremely accurate at detecting relatively recent demographic events when applied to a long stretch of highly polymorphic, well-characterized DNA and corrected for time-dependent variation in mutation rates. To our knowledge, differences in population growth between agriculturalist and hunter-gatherer lineages from the same region have not been directly measured before using genetic data. Using genetic data from European, sub-Saharan African, and southeastern Asian populations, we reconstruct demographic fluctu-

ations over the past 50,000 y. Estimates of the timing of rapid population growth during the Holocene strongly correlate with established archaeological dates for the adoption and innovation of agricultural practices (Fig. 1). Holocene-period population expansions were approximately five times faster than earlier modern human periods. Even during the Holocene, genetic lineages associated with indigenous hunter-gatherers do not show the same dramatic expansion as those associated with agriculture. Although the initial stimuli for the origins of early agriculture appear to be complex, changing modes of food production facilitated a novel capacity for exceptional human population growth.

Materials and Methods

Coalescent Analysis. We took advantage of previously published mitochondrial phylogeographic studies, based on limited sequence data, to gain prior information for building models with larger datasets. To uncover multiple episodes of demographic growth during human prehistory we assembled a dataset of 425 mtDNA sequences. Representatives of different haplogroups were included in each sample set to avoid lineage-specific effects. Where possible, haplogroups derived from both the M and N lineages were chosen. We used the BEAST program to create Bayesian Skyline plots, which measure demographic changes in a population via the relative number of coalescent events for serial time periods. Each was run for 40 million steps, well above what is minimally required (16, 21). Runs were only repeated to refine Skyline parameters for acceptable effective sample sizes values (i.e., >100). Timing of the population growth was calibrated according to a time-dependent curve of mutation rate decline to obtain more accurate dates (38) (see below). We assumed an average female generation time of 30 y (39).

Calibration of Coding Region Mutation Rates. Mitochondrial mutation rate estimates are subject to a time-dependent decay over evolutionary timescales, as pedigree-based rate estimates can be 10-fold faster than phylogenetic-based rate estimates. In prior work (17), we showed that coding region substitution rates varied with time in a two-phase process: first, following a first-order decay from the pedigree mutation rate, and then approaching an equilibrium phylogenetic rate. We fit the coding region sequence estimates from Henn et al. (17) by using a least-squares method of residuals to characterize both phases of the mutation rate using the same equation. For the equilibrium mutation rate (after the within-human rate decay has occurred), we estimated the human-chimpanzee phylogeny-based rate at 1.28×10^{-8}/bp·yr^{-1}, consistent with other estimates of full coding region sequence (40, 41) but scaled to a human-chimpanzee divergence of 6.5 million ya. The mutation rates were calibrated by using archaeological dates for first colonization events (e.g., such as the colonization of Polynesia and Taiwan). Mutation rates obtained in this manner incorporate the effects of purifying selection and demography because they are based on actual, empirical estimates.

To calibrate each coalescent event to the correct time-dependent mutation rate, we first estimated an approximate time interval "t" for a given genetic MRCA "d" by ($t = d/\mu_{hc}$) where the approximate mutation rate is the human-chimpanzee rate ($\mu_{hc} = 1.28 \times 10^{-8}$/bp·yr^{-1}). Then, assuming the estimated t, we adjusted the mutation rate using the equation below, where μ_{cal} indicates the adjusted mutation rate.

$$\mu_{cal} = 1.28 \times 10^{-8} + 1.73 \times 10^{-8}\left(e^{-4.72 \times 10^{-5} t}\right)$$

Using the adjusted rate, we can then estimated a calibrated time of divergence:

$$t_{cal} = d/\mu_{cal}$$

Several papers have suggested evidence for selective pressures on the mitochondrial genome (42). Our selection of datasets for skyline analysis minimizes lineage-specific biases and, indeed, we saw no evidence from the BEAST output to reject our null hypothesis of a homogeneous clock across branches. Modeling the coalescent in this manner does not allow for testing of a systematic mutational rate slowdown across all lineages, so it is better to account for the changing mutation rate via postprocessing of the BEAST estimates by using the process above.

Population Growth Rate Calculations. Using the population growth curves generated from BEAST (see above), we calculated the rate of population growth per year. Each Skyline plot consisted of 100 smoothed data points, at ≈300–500 y intervals. For the Holocene period, population size increase was preceded by a brief period of stationary size or even decrease. The initial population size N_0 was set as the minimum population size during the period immediately preceding population growth. For the Upper Paleolithic and LGP skyline plots, population size tended to increase very slowly for thousands of years before the punctuated growth curve. We therefore chose the interval when population size began to increase significantly by visual examination. We also estimated the population growth rate for the interval in our data where growth was the fastest (Table 1). We chose the exponential growth equation rather than a logistic growth equation for this analysis:

$$r = \frac{\ln(N_t/N_0)}{t}$$

where "r" represents the population growth rate per year, "N_0" is the initial population size and t the amount of time since growth began. The logistic growth equation incorporates a carrying capacity parameter "K" and it is unclear how carrying capacity should be interpreted from coalescent analysis of growth curves when multiple groups of individuals are occupying the same niche.

ACKNOWLEDGMENTS. We thank Marcus Feldman and Richard Klein for their detailed comments on our manuscript and J Michael Macpherson and Sohini Ramachandran for stimulating discussion. We acknowledge funding from National Institutes of Health Grant T32-GM07175 (to Francis Szoka, Jr.), the UCSF Chancellor's Graduate Research Fellowship (to C.R.G.), and the Institute of Human Origins, Stanford University, Departments of Anthropology and Biological Sciences (to B.M.H.).

1. Diamond J, Bellwood P (2003) Farmers and their languages: The first expansions. *Science* 300:597–603.
2. Haak W, et al. (2005) Ancient DNA from the first European farmers in 7500-year-old Neolithic sites. *Science* 310:1016–1018.
3. Bramanti B, et al. (2009) Genetic discontinuity between local hunter-gatherers and central Europe's first farmers. *Science* 326:137–140.
4. Chikhi L, Nichols RA, Barbujani G, Beaumont MA (2002) Y genetic data support the Neolithic demic diffusion model. *Proc Natl Acad Sci USA* 99:11008–11013.
5. Dupanloup I, Bertorelle G, Chikhi L, Barbujani G (2004) Estimating the impact of prehistoric admixture on the genome of Europeans. *Mol Biol Evol* 21:1361–1372.
6. Currat M, Excoffier L (2005) The effect of the Neolithic expansion on European molecular diversity. *Proc R Soc Lond B Biol Sci* 272:679–688.
7. Richards M, et al. (2000) Tracing European founder lineages in the Near Eastern mtDNA pool. *Am J Hum Genet* 67:1251–1276.
8. Arredi B, et al. (2004) A predominantly neolithic origin for Y-chromosomal DNA variation in North Africa. *Am J Hum Genet* 75:338–345.
9. Cordaux R, Deepa E, Vishwanathan H, Stoneking M (2004) Genetic evidence for the demic diffusion of agriculture to India. *Science* 304:1125.
10. Wen B, et al. (2004) Genetic evidence supports demic diffusion of Han culture. *Nature* 431:302–305.
11. Macpherson JM, Ramachandran S, Diamond L, Feldman MW (2004) Demographic estimates from Y chromosome microsatellite polymorphisms: analysis of a worldwide sample. *Hum Genomics* 1:345–354.
12. Atkinson QD, Gray RD, Drummond AJ (2008) mtDNA variation predicts population size in humans and reveals a major Southern Asian chapter in human prehistory. *Mol Biol Evol* 25:468–474.
13. Pritchard JK, Seielstad MT, Perez-Lezaun A, Feldman MW (1999) Population growth of human Y chromosomes: A study of Y chromosome microsatellites. *Mol Biol Evol* 16: 1791–1798.
14. Xue Y, et al. (2006) Male demography in East Asia: A north-south contrast in human population expansion times. *Genetics* 172:2431–2439.
15. Kitchen A, Miyamoto MM, Mulligan CJ (2008) A three-stage colonization model for the peopling of the Americas. *PLoS ONE* 3:e1596.
16. Drummond AJ, Rambaut A (2007) BEAST: Bayesian evolutionary analysis by sampling trees. *BMC Evol Biol* 7:214.
17. Henn BM, Gignoux CR, Feldman MW, Mountain JL (2009) Characterizing the time dependency of human mitochondrial DNA mutation rate estimates. *Mol Biol Evol* 26: 217–230.
18. Ho SYW, Endicott P (2008) The crucial role of calibration in molecular date estimates for the peopling of the Americas. *Am J Hum Genet* 83:142–146, author reply 146–147.
19. Atkinson QD, Gray RD, Drummond AJ (2009) Bayesian coalescent inference of major human mitochondrial DNA haplogroup expansions in Africa. *Proc R Soc Lond B Biol Sci* 276:367.
20. Campos PF, et al. (2010) Ancient DNA analyses exclude humans as the driving force behind late Pleistocene musk ox (Ovibos moschatus) population dynamics. *Proc Natl Acad Sci USA* 107:5675–5680.
21. Drummond AJ, Rambaut A, Shapiro B, Pybus OG (2005) Bayesian coalescent inference of past population dynamics from molecular sequences. *Mol Biol Evol* 22:1185–1192.

22. Underhill PA, Kivisild T (2007) Use of Y chromosome and mitochondrial DNA population structure in tracing human migrations. *Annu Rev Genet* 41:539–564.
23. Pinhasi R, Fort J, Ammerman AJ (2005) Tracing the origin and spread of agriculture in Europe. *PLoS Biol* 3:e410.
24. Isarin RFB, Renssen H (1999) Reconstructing and modelling Late Weichselian climates: the Younger Dryas in Europe as a case study. *Earth Sci Rev* 48:1–38.
25. Auton A, et al. (2009) Global distribution of genomic diversity underscores rich complex history of continental human populations. *Genome Res* 19:795–803.
26. Forster P (2004) Ice Ages and the mitochondrial DNA chronology of human dispersals: A review. *Philos Trans R Soc Lond B Biol Sci* 359:255–264, discussion 264.
27. Phillipson DW (2005) *African Archaeology* (Cambridge Univ Press, Cambridge, UK).
28. Glover IC, Higham CFW (1996) *The Origins and Spread of Agriculture and Pastoralism in Eurasia*, ed Harris DR (Routledge, Oxon, UK), pp 413–440.
29. Denham T (2003) Archaeological evidence for mid-holocene agriculture in the interior of Papua New Guinea: A critical review. *Archaeology in Oceania* 38:159–176.
30. Friedlaender JS, et al. (2007) Melanesian mtDNA complexity. *PLoS ONE* 2:e248.
31. Fairbairn A, Hope G, Summerhayes G (2006) Pleistocene occupation of New Guinea's highland and subalpine environments. *World Archaeol* 38:371–386.
32. Tang H, Siegmund DO, Shen P, Oefner PJ, Feldman MW (2002) Frequentist estimation of coalescence times from nucleotide sequence data using a tree-based partition. *Genetics* 161:447–459.
33. Ammerman AJ, Cavalli-Sforza LL (1984) *The Neolithic Transition and the Genetics of Populations in Europe* (Princeton Univ Press, Princeton, NJ).
34. D'Andrea AC, Casey J (2002) Pearl millet and Kintampo subsistence. *Afr Archaeol Rev* 19:147–173.
35. Zhivotovsky LA, Rosenberg NA, Feldman MW (2003) Features of evolution and expansion of modern humans, inferred from genomewide microsatellite markers. *Am J Hum Genet* 72:1171–1186.
36. Marth GT, Czabarka E, Murvai J, Sherry ST (2004) The allele frequency spectrum in genome-wide human variation data reveals signals of differential demographic history in three large world populations. *Genetics* 166:351–372.
37. Voight BF, et al. (2005) Interrogating multiple aspects of variation in a full resequencing data set to infer human population size changes. *Proc Natl Acad Sci USA* 102:18508–18513.
38. Henn BM, et al. (2008) Y-chromosomal evidence of a pastoralist migration through Tanzania to southern Africa. *Proc Natl Acad Sci USA* 105:10693–10698.
39. Tremblay M, Vézina H (2000) New estimates of intergenerational time intervals for the calculation of age and origins of mutations. *Am J Hum Genet* 66:651–658.
40. Ingman M, Kaessmann H, Pääbo S, Gyllensten U (2000) Mitochondrial genome variation and the origin of modern humans. *Nature* 408:708–713.
41. Mishmar D, et al. (2003) Natural selection shaped regional mtDNA variation in humans. *Proc Natl Acad Sci USA* 100:171–176.
42. Kivisild T, et al. (2006) The role of selection in the evolution of human mitochondrial genomes. *Genetics* 172:373–387.